Endless Polarization Control Systems for Coherent Optics

REINHOLD NOÉ, HELMUT HEIDRICH, AND DETLEF HOFFMANN

***Abstract*—In coherent optical systems or sensors, polarization matching between the superposed beams must be assured. The tracking range of automatic polarization control systems should be endless, i.e., any resets of finite range retarders, which transform the polarization, should cause no significant intensity losses. A variety of experimental systems including a computer as feedback controller are described in this paper. They include the minimum configuration of three fixed eigenmode retarders, i.e., the orientation of birefringence cannot be changed. These retarders are realized by fiber squeezers. Error-tolerant systems which contain more than the minimum number of elements, however, are better suited to cope with time variant retarder transfer functions, etc. A fourth fiber squeezer allows the losses of a nonideal system to be kept to only 0.07 dB. Finally for the first time a closed loop system with two integrated optical retarders is described. These retarders have variable eigenmodes, i.e., adjustable birefringence orientation. An optimization procedure helps to idealize the device behavior. The system has less than 0.15 dB intensity losses, coupling and attenuation not included.**

I. Introduction

COHERENT optical transmission systems improve the receiver sensitivity and allow a close spacing of several channels on one fiber [1]–[6]. However, as in fiber-optic sensors, polarization matching between the two superposed waves must be achieved by some means. The "classical" method considered in this paper is automatic polarization control at the receiver [7]. Polarization diversity receivers now offer almost equal receiver sensitivity at the expense of two receiver front ends [8]–[11], whereas polarization scrambling [12] reduces the receiver sensitivity. The simplest possibility is the use of polarization maintaining fibers [13], but problems may arise from fiber attenuation and splicing.

The state-of-polarization (SOP) at the end of a long conventional single-mode fiber is subject to slow but potentially large changes. To ensure reliable communication without interruptions, the tracking range of the polarization control system should be endless. In Section II-E, an experiment will be shown which underlines this necessity.

Generally SOP control systems contain one or several retarders, i.e., birefringent elements. They transform the incident SOP by imposing a phase delay between one fundamental polarization mode, which is subsequently referred to as an eigenmode, and the orthogonal eigenmode. Section II describes systems with retarders whose retardations or amounts of birefringence are changed electrically but whose eigenmodes or orientations of birefringence remain fixed. Section III deals with systems containing variable eigenmode retarders, i.e., the orientations of birefringence may also be changed like in rotatable waveplates. The work in this paper has partly been presented in [8] and [14]–[16].

Manuscript received July 27, 1987; revised November 10, 1987. This work was partially supported by the Federal Ministry of Research and Technology of the F.R.G. and by Siemens AG.

R. Noé was with Siemens AG, Munich, F.R.G. He is now with Bellcore, Red Bank, NJ 07701.

H. Heidrich and D. Hoffman are with the Heinrich-Hertz-Institut für Nachrichtechnik Berlin GmbH, Berlin, F.R.G.

IEEE Log Number 8820877.

II. Systems with Retarders of Fixed Eigenmodes

A. Description of Polarization and Retarders

The 2 × 1 Jones vectors and 2 × 2 Jones matrices [17] are widely used for the description of polarization, whereas the Poincaré sphere [18] provides easy insight into problems. Both formulations shall be used in this paper.

The electrical field of a lightwave at a fixed point can be expressed by the complex vector

$$\vec{E}(t) = \begin{bmatrix} E_x(t) \\ E_y(t) \end{bmatrix} = \begin{bmatrix} E_x \\ E_y \end{bmatrix} \cdot \exp(j\omega t) = \vec{E} \cdot \exp(j\omega t) \tag{1}$$

where $\vec{E} = [E_x, E_y]^T$ is the (x, y) Jones vector for the orthogonal polarization components in x- and y-directions. In an optical heterodyne or homodyne receiver the signal and local oscillator fields $\vec{E}_S$ and $\vec{E}_{LO}$ are superposed in a coupler and squared at the detector. The photocurrent is

$$\begin{aligned} i(t) &= c \cdot \left|\vec{E}_S(t) + \vec{E}_{LO}(t)\right|^2 \\ &= c \cdot \left\{\left|\vec{E}_S\right|^2 + \left|\vec{E}_{LO}\right|^2 + 2 \cdot \left|\vec{E}_S \cdot \vec{E}^*_{LO}\right| \right. \\ &\quad \left. \cdot \cos(\omega_{IF} t + \varphi_{IF})\right\} \end{aligned} \tag{2}$$

where

$$\omega_{IF} = \omega_S - \omega_{LO}$$

$$\sin(\varphi_{IF}) = \mathrm{Im}(\vec{E}_S \cdot \vec{E}^*_{LO}) / \left|\vec{E}_S \cdot \vec{E}^*_{LO}\right|$$

$$\cos(\varphi_{IF}) = \mathrm{Re}(\vec{E}_S \cdot \vec{E}^*_{LO}) / \left|\vec{E}_S \cdot \vec{E}^*_{LO}\right|.$$

The constant c depends on the field distributions, wavelength, and quantum efficiency of the detector. The normalized electrical power of the IF signal is now defined

0733-8724/88/0700-1199$01.00 © 1988 IEEE

as the intensity I:

$$I = \frac{|\vec{E}_S \cdot \vec{E}^*_{LO}|^2}{|\vec{E}_S|^2 \cdot |\vec{E}_{LO}|^2}. \quad (3)$$

Put another way, a lightwave $\vec{E}_S$ has the normalized power I after passing through an elliptical polarizer which has the transmitted eigenmode $\vec{E}_{LO}$. The Poincaré sphere (Fig. 1) uniquely represents each SOP by a point on its surface. The equator carries all linear SOP's like horizontal H and vertical V. P and Q are inclined by $\pm 45°$ to the horizontal. The poles refer to right R and left L circular polarization. An elliptical SOP has a major axis azimuth α and ellipticity $\beta = \arctan(b/a)$ where b and a are the minor and major axes, respectively. On the sphere this is represented by the spherical coordinates 2α and 2β. The equivalent to (3) is

$$I = \cos(\widehat{P_S P_{LO}}/2)^2. \quad (4)$$

where $\widehat{P_S P_{LO}}$ is the angle between the corresponding points on the sphere. If a lightwave passes through a retarder or birefringent medium, its SOP is generally altered. Only two SOP's, the eigenmodes, remain unchanged. A linear retarder with horizontal and vertical linear eigenmodes is represented by the Jones matrix (transition matrix for the Jones vector):

$$\boldsymbol{L}(0°, d) = \begin{bmatrix} \exp(jd/2) & 0 \\ 0 & \exp(-jd/2) \end{bmatrix},$$

$$\text{eigenmodes} \begin{bmatrix} 1 \\ 0 \end{bmatrix}, \quad \text{and} \begin{bmatrix} 0 \\ 1 \end{bmatrix} \quad (5)$$

where d is the phase difference or retardation between the eigenmodes. On the Poincaré sphere this retarder (type A) transforms the incident SOP by an anticlockwise turn of angle d around the HV axis. Examples for this linear retarder are fiber squeezers [19], [20] with 0° azimuth or, in integrated optics, phase shifters [21], [22].

A linear retarder whose eigenmodes are inclined by $\pm 45°$ with respect to the horizontal (type B) is given by:

$$\boldsymbol{L}(45°, d) = \begin{bmatrix} \cos(d/2) & j \cdot \sin(d/2) \\ j \cdot \sin(d/2) & \cos(d/2) \end{bmatrix},$$

$$\text{eigenmodes } 1/\sqrt{2} \begin{bmatrix} 1 \\ 1 \end{bmatrix},$$

$$\text{and } 1/\sqrt{2} \begin{bmatrix} 1 \\ -1 \end{bmatrix}. \quad (6)$$

Such a retarder turns any SOP around the PQ axis. Fiber squeezers of 45° azimuths or integrated optical TE/TM convertors [21], [22] may be used. Other types of retarders are the circular retarder (type C), e.g., realized by Faraday rotators or a rotation of the coordinate system, or in the general case the elliptical retarder. One retarder type can be realized by another type if it is placed between two retarders of the third type which have $\pm\pi/2$ retardation [19]. For example, a fiber squeezer with 45° azimuth (type B) may be looked upon as fiber squeezer of 0° azimuth (type A) between two fiber sections in which the coordinate system is rotated by $\pm 45°$, corresponding to $\pm\pi/2$ circular retardation (type C). If a lightwave passes through a retarder, the intensity defined by (3) or (4) can be shown to vary sinusoidally as a function of the retardation d. If the input SOP of the retarder or the input SOP analyzed beyond the retarder is an eigenmode, then the intensity will stay constant. If both SOPs are eigenmodes, the intensity will stay constant either at 0 or 1.

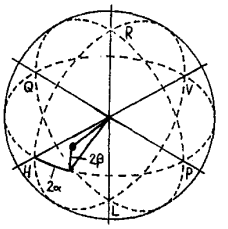

Fig. 1. Poincaré sphere.

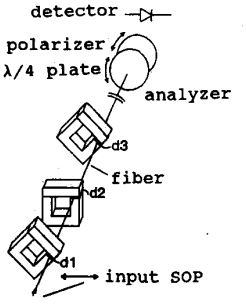

Fig. 2. Experimental setup with 3 fiber squeezers and SOP analyzer.

B. Operation Principle of a Three Retarder System

It shall be assumed now that the SOP controllers are entirely situated between the LO and the (polarization insensitive) coupler. The SOP of the LO may be unknown but is certainly constant. (Experimental systems which can deal with both varying input and output SOP's are described in [23]–[25].) The polarization controllers can also be placed between the coupler and the receiver input, if their order in the light path is inverted.

The first proposal for an endless polarization control system employed four retarders [26] of all three types. The first experimental system [16], [23], [24] had four retarders of only types A and B. It was tried out both in a heterodyne transmission system and in an arrangement with one laser and a variable SOP analyzer. No fundamental differences were observed between the two setups. Meanwhile polarization control systems with only three retarders of two types have been proposed [14], [27]. The experimental system [14] shall now be described in detail. It uses one of three possible reset algorithms. Many other retarder configurations and retardation range limits are possible.

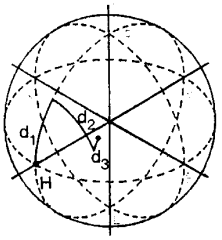

Fig. 3. SOP transformations of the 3 retarder system on the Poincaré sphere.

The configuration is sketched in Fig. 2, a set of SOP transformations is shown in Fig. 3. The horizontal input SOP (Jones vector $[1, 0]^T$) is transformed by three retarders of retardations d_1, d_2, d_3 and of types B, A, B, respectively. The output SOP is given by matrix multiplications as

$$\vec{E}(d_1, d_2, d_3) = \boldsymbol{L}(45°, d_3) \cdot \boldsymbol{L}(0°, d_2) \cdot \boldsymbol{L}(45°, d_1) \cdot \begin{bmatrix} 1 \\ 0 \end{bmatrix}$$

$$= \begin{bmatrix} \cos(d_3/2) \cdot \exp(jd_2/2) \cdot \cos(d_1/2) - \sin(d_3/2) \cdot \exp(-jd_2/2) \cdot \sin(d_1/2) \\ j \cdot \sin(d_3/2) \cdot \exp(jd_2/2) \cdot \cos(d_1/2) + j \cdot \cos(d_3/2) \cdot \exp(-jd_2/2) \cdot \sin(d_1/2) \end{bmatrix}. \quad (7)$$

If the third retarder is absent or $d_3 = 0$, (7) simplifies to

$$\vec{E}(d_1, d_2, 0) = \begin{bmatrix} \exp(jd_2/2) \cdot \cos(d_1/2) \\ j \cdot \exp(-jd_2/2) \cdot \sin(d_1/2) \end{bmatrix}. \quad (8)$$

The retardation ranges are now chosen between the limits $k\pi$ and $(k + 1)\pi$ for d_1 and between the limits $i\pi$ and $(i + 2)\pi$ for d_2, where k, i are integers. The choice allows generation of any desired output SOP. This fact is also true with the third retarder present. The polarization matching may conveniently be implemented by an automatic control system which modulates ("dithers") d_1 and d_2 around the operation points. The corresponding intensity fluctuations given by (8) or (7) and (3) allow one to determine the intensity gradient, i.e., the partial derivatives $\partial I/\partial d_i$ with respect to the retardations. Integral controllers change the operation points in the direction of increasing intensity to achieve best matching $I = 1$. Alternatively, if the direction of the gradient is inverted, the system will lock onto $I = 0$. This minimum is not desired for optical communications but is useful to check for small intensity losses while being insensitive to optical power fluctuations.

The endlessness of the tracking range is established by the following equations which hold at the properly chosen d_1 and d_2 range limits:

$$\vec{E}(k\pi, d_2 + x, d_3) = \exp\left(j(-1)^k \cdot x/2\right) \cdot \vec{E}(k\pi, d_2, d_3) \quad (9)$$

$$\vec{E}(k\pi + x, d_2 \pm \pi, d_3) = j \cdot (-1)^k \cdot \vec{E}(k\pi - x, d_2, d_3) \quad (10)$$

$$\vec{E}(d_1 - (-1)^i x, i\pi, d_3 + x) = \vec{E}(d_1, i\pi, d_3). \quad (11)$$

These equations mean that the generated SOP theoretically will not change if the retardations are changed by appropriate reset procedures. Only the light phase may change, which does not deteriorate the function of the optical receiver, as long as the phase changes are slow compared to the bit rate.

If d_1 reaches a range limit, e.g., the point $k\pi$, the SOP is not altered by any variations of d_2 (9), because it is an eigenmode. If d_1 has passed the point $k\pi$, d_2 is incremented or decremented by π. The direction is chosen so as not to exceed the d_2 range. As the desired effect this action mirrors the d_1-scaling at the range limit $k\pi$ (10). If the tracking system has just moved d_1 beyond the range limit, d_1 will return subsequently within the range.

As an alternative d_1 may simply be limited slightly before reaching the nominal range limit. In this case small areas around the points H and V of the Poincaré sphere are not accessible by the system. Meanwhile the intensity optimization algorithm will find out how to change d_2 for the best intensity.

If d_2 reaches a range limit, e.g., the point $i\pi$, the reset procedure is more complicated. First d_1 and d_3 simultaneously move in opposite (if i is even) or equal (if i is odd) directions until d_1 reaches the nearest range limit (11). During this operation d_3 takes over the function of d_1. The SOP at the second retarder becomes one of its eigenmodes and d_2 may be changed (9) by 2π away from the range limit, i.e., to the other range limit $(i + 2)\pi$. At the end d_1 and d_3 are simultaneously led back to their former operation points (11).

Frequent resets or system blocking are prevented by an appropriate switching hysteresis at the range limits.

C. Experiments with a Three Retarder System

A three retarder system was built using a 1523-nm HeNe-laser source and a variable SOP analyzer (Fig. 2). A desktop computer worked as feedback-controller. The transfer functions of the retarders were accurately determined by an automatic calibration program. It records sine-like and cosine-like intensity, functions versus magnet current for the fiber squeezers and calculates the corresponding retardations. The total insertion loss of all devices is about 0.1 dB. Intensity optimization is carried out by a gradient algorithm acting on d_1 and d_2. One iteration took about 0.1 s per retardation. The modulation amplitudes are adaptively modified to produce constant intensity losses of 0.05 dB ($\triangleq 0.01$). If desired, this value can be improved by averaging several modulation cycles. One

cycle required 5 ms for each component. The modulation steps are not shown in the following figures.

Fig. 4 shows the system behavior with rotating polarizer. d_1 varied in a periodic, sine-like movement, whereas the d_2 movement was a ramp. If d_2 reached the lower range limit π the above described reset procedure was carried out. The intensity losses were only about 0.4 dB. At the right hand side of the figure the polarizer was stopped and d_2 was manually reset by 2π without changing d_1 or d_3. This would be the procedure in a conventional, nonendless SOP control system. A strong intensity dip indicates that a data transmission system would have suffered error rate bursts.

To improve the system the conventional fiber between the magnet poles was replaced by low birefringence fiber (York) and the input SOP near the horizontal point was better adjusted. Now the intensity losses dropped to 0.1 dB as shown in Fig. 5. The polarizer and the quarter wave plate were moved back and forth so as to produce frequent d_2 resets which had different d_1 values as starting points.

In most cases d_1 does not reach its range limits. It will do so only if the required SOP crosses the points H or V of the Poincaré sphere. To do so, the quarter wave plate had to be carefully adjusted. In the left and right part of Fig. 6 the polarizer rotates, respectively, in opposite directions. The intensity was minimized to show the actual losses. Zero intensity corresponds to the very low photo current which is observed if the SOP analyzer were set orthogonal to the incident SOP. The best results were obtained if d_1 was limited 0.1 rad before each range limit. The intensity minimization [28] automatically changes d_2 about π which makes d_1 return from the range limits. If the d_2 range is exceeded the appropriate reset is carried out, this time faster than in Figs. 4 and 5. The intensity losses are below 0.05 dB.

The experiments proved that unlimited, endless SOP changes may be tracked with intensity losses of only 0.1 dB. However, the comparison of Figs. 4 and 5 shows that the intensity losses increase strongly in the presence of nonideal input SOP (not horizontal or vertical), time variant retardation characteristics of the fiber squeezers or unwanted variations of their eigenmodes as function of the retardations. This kind of effect is especially encountered [8] when using integrated optical retarders. To ensure a certain ruggedness it is therefore desirable to have a redundant or error-tolerant system. It accurately controls the SOP even during the critical resets and thus will need more than the minimum number of retarders.

D. Operation Principle of an Error-Tolerant Four Retarder System

The system of Sections II-B and II-C is made error-tolerant by adding another type A retarder of retardation d_0 at the SOP transformer input (Fig. 7). The retardation range of d_1 including range limits must be transferred by $\pi/2$. The SOP transformations are shown in Fig. 8 which is directly comparable to Fig. 3. The input SOP is no longer horizontal but linear in 45° direction (point P_0).

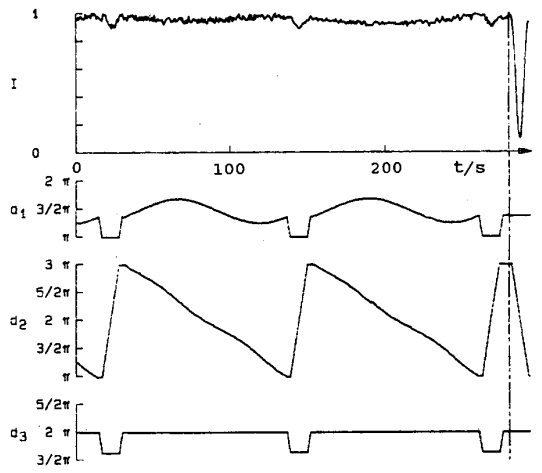

Fig. 4. Intensity and retardations for an endless SOP control with d_2 resets caused by rotating polarizer.

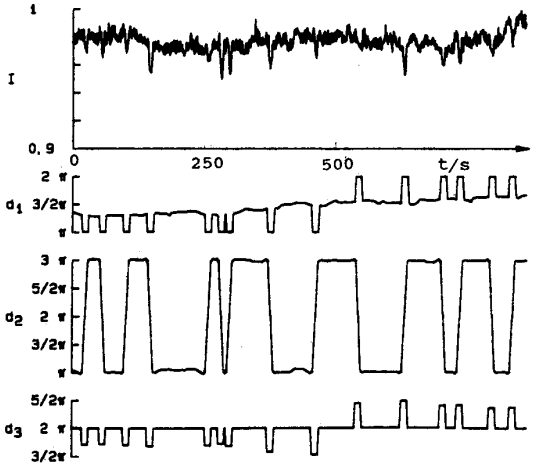

Fig. 5. d_2 resets from different d_1 starting points.

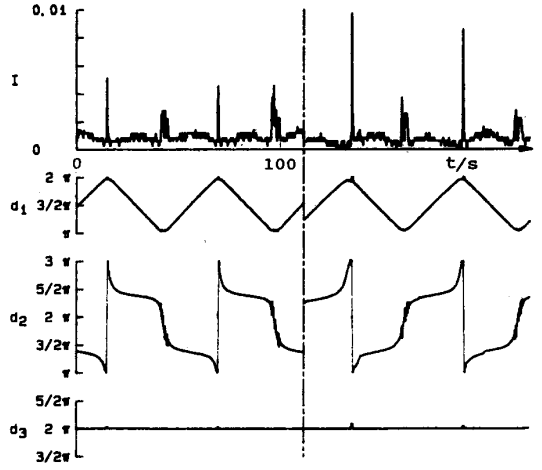

Fig. 6. Endless SOP control with d_1 resets caused by rotating polarizer.

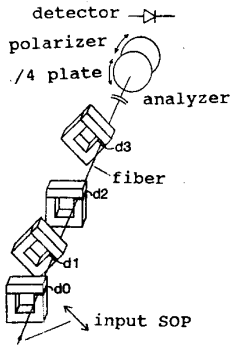

Fig. 7. Experimental setup of the error-tolerant 4 retarder system.

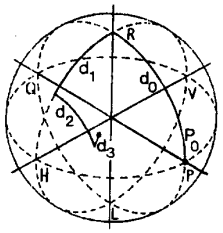

Fig. 8. SOP transformations of the error-tolerant system on the Poincaré sphere.

The intensity losses in Figs. 4–6 are due to changes in the output SOP during the resets. In the general case they occur in both dimensions of the Poincaré sphere surface.

Unlike before, this system modulates all four retardations. Integral controllers act on d_1 and d_2 which theoretically can generate any desired output SOP. Nonideal system behavior such as imperfect optical elements or input polarization deviations might prevent the system from exactly reaching all required SOP's. Additional proportional first order low-pass controllers acting on d_0 and d_3 overcome this problem. The mean operation point of d_3 is arbitrarily fixed to 0.

The reset operations are almost the same as in the three-retarder system. The range limits of d_1 are $(k - 1/2)\pi$ and $(k + 1/2)\pi$. The corresponding SOP's H and V of Fig. 8 are the d_2 eigenmodes. If d_1 has passed one of these points, d_2 is slowly incremented or decremented by π. During the reset the SOP is accurately controlled via d_0 and d_1 which are then switched over to integral controllers. The two retardations may transfer the generated SOP in any direction by small amounts. Consequently the gradient algorithm is able to keep the intensity continuously at its maximum. As the d_1 scaling is mirrored during the reset, the direction of movement reverses and d_1 will return from the range limit.

At the beginning of a d_2 reset, d_3 takes over the function of d_1. To correct system errors, d_0 and d_3 are acted on by integral controllers. While d_2 is changed by 2π, integral controllers for d_0 and d_1 correct output SOP deviations. When d_1 and d_3 are moved back to their former operation points, d_0 and d_3 once again control the generated SOP. Then the system switches back to normal operation.

E. Experiments with an Error-Tolerant Four Retarder System

During the following measurements, the SOP P_0 at the transformer input is deliberately adjusted not to point P (or Q), but deviates by 0.3 rad on the sphere. In this manner system imperfections are continuously present in spite of quasi-ideal fiber squeezers.

Fig. 9(a) shows once more the unacceptable signal behavior of a conventional polarization control system if d_2 is reset by 2π without special precautions. Fig. 9(b) corresponds to the three-retarder system which does not control the SOP during the resets. Some losses occur because the output SOP deviates from its initial value due to the nonideal input SOP and other system errors. In Fig. 9(c) finally the output SOP is continuously controlled during the reset and the signal stays at its maximum.

To investigate the remaining losses, the intensity was minimized as shown in Fig. 10. The analyzed SOP is changed and several resets occur at different d_1 operation points. The worst signal loss is only 0.02 dB, to which the modulation loss of 0.05 dB must be added.

Finally 4.4 km of fiber on two reels was inserted between the output of the SOP transformer and the analyzer. The intensity was maximized as in a real coherent transmission system (Fig. 11). The fiber was heated by 40 K in 15 min. The system performs resets of d_2 and also of d_1, which proves the necessity of endless polarization control. The hysteresis at each d_1 range limit are as large as 0.3 rad. This makes d_1 return well within the range when d_2 is changed by π during a reset. The signal fluctuations of 0.3 dB are due to varying coupling efficiencies and reflections, not to SOP mismatch. The real signal loss may be roughly estimated from the maximum changing speeds of d_1, d_2, about 0.1 rad per iteration, and lies within 0.02 dB.

As expected, d_0 and d_3 range overflows were never observed. The error-tolerant four retarder system has only negligible intensity losses and offers a performance superior to that of the three retarder system at the expense of reduced control speed.

III. System with Retarders of Variable Eigenmodes

A. Fiber-Optic Versions

Quarter-wave and half-wave plates are well known to allow SOP transformation. Rotatable fiber coils [29] are widely used as the fiber-optic equivalents of waveplates. The first endless SOP control devices derived from this scheme are fiber cranks [30] or coils [31], [32] which can be rotated endlessly without breaking the fiber. However, they seem not to be free from mechanical fatigue and the expense of mechanics is considerable.

B. Operation Principle and Realization of Integrated Optical (IO) Devices

The function of an endless polarization control system with integrated optical retarders of variable linear eigen-

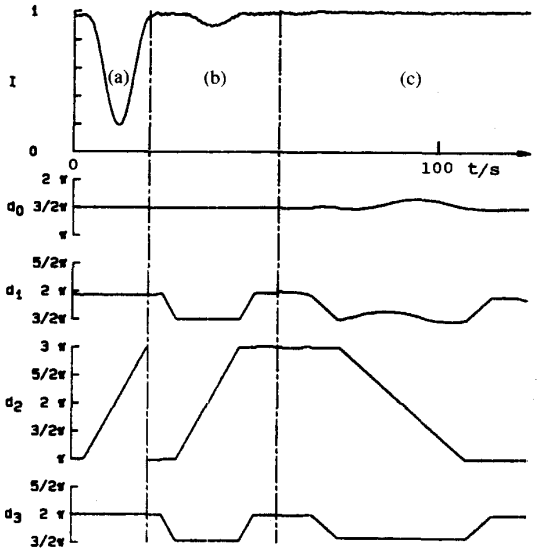

Fig. 9. Intensity and retardations in (a) conventional and (b), (c) endless control systems including resets.

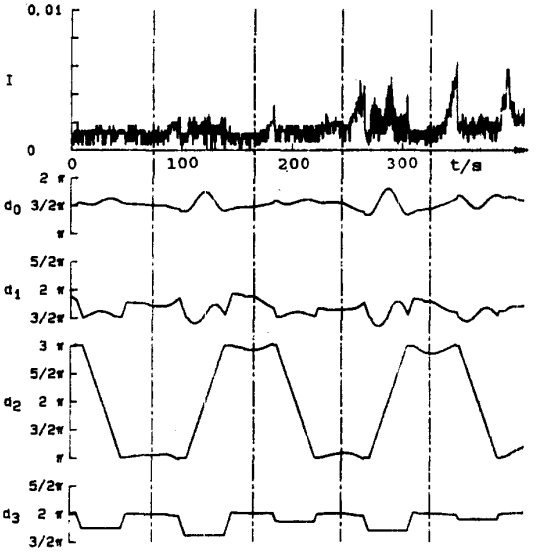

Fig. 10. Intensity losses of the error-tolerant system at different resets.

modes is best described by circular vectors and matrices [17]. They use left and right circular polarizations (L and R) as vector basis instead of horizontal and vertical (H and V). The circular Jones matrix $\boldsymbol{T}_{l,r}$ of a general linear retarder takes the simple form

$$\boldsymbol{T}_{l,r} = \begin{bmatrix} \cos(d_1/2) & j \cdot \exp(jd_2) \cdot \sin(d_1/2) \\ j \cdot \exp(-jd_2) \cdot \sin(d_1/2) & \cos(d_1/2) \end{bmatrix} \tag{12}$$

where d_1 is now the retardation between the linear eigenmodes. Their azimuth angles are $d_2/2$ and $d_2/2 + \pi/2$ with respect to the horizontal. The input polarization is chosen circular, e.g., right circular. The output SOP

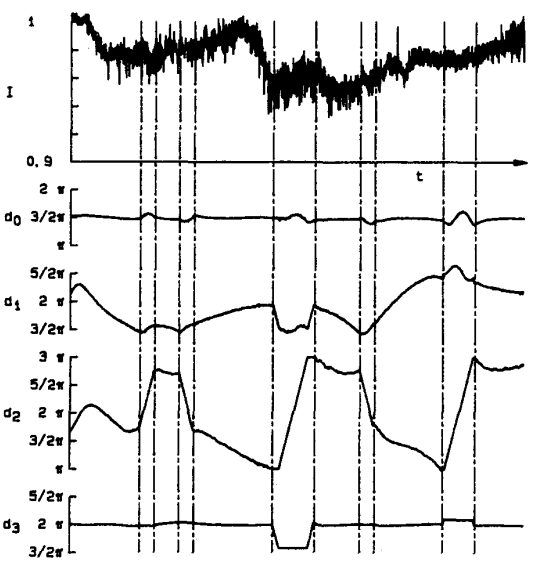

Fig. 11. Control of SOP fluctuations from a 4.4-km-long single-mode fiber.

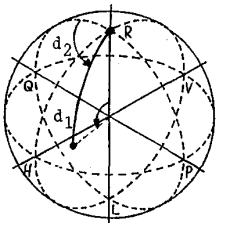

Fig. 12. SOP transformations on the Poincaré sphere for the retarder starting with circular input SOP.

$\vec{E}_{l,r}$ in circular coordinates becomes

$$\vec{E}_{l,r} = \boldsymbol{T}_{l,r} \cdot \begin{bmatrix} 0 \\ 1 \end{bmatrix} = \begin{bmatrix} \cos(d_1/2) \\ j \cdot \exp(-jd_2) \cdot \sin(d_1/2) \end{bmatrix}. \tag{13}$$

To achieve endless SOP control, the range of d_1 is chosen from 0 to π and the double azimuth d_2 must be endlessly rotatable. Fig. 12 shows SOP transformations on the Poincaré sphere. It should be pointed out that in theory one single retarder is sufficient for endless polarization control, including resets.

Apart from SOP control such a device can be used as endless phase shifter or frequency translator for positive and negative frequencies if $d_1 = \pi$. d_2 performs the desired phase shift on the circularly polarized output light. This device has already been realized in bulk optics [33]. It is less complicated than a similar IO proposal [34] at the expense of higher driving voltages.

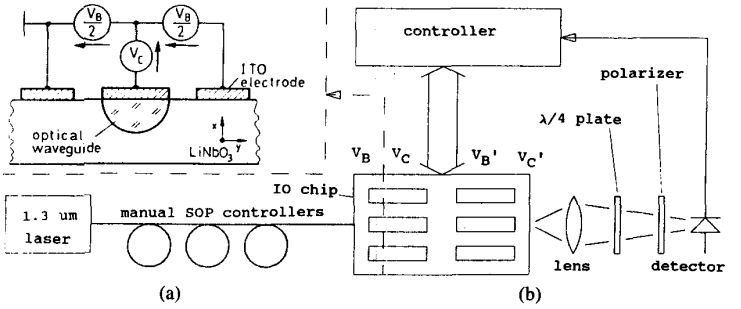

Fig. 13. Cross section of an integrated optical retarder (a) waveguide and electrodes and (b) experimental setup with two retarders.

Such linear retarders have been realized as IO versions on a lithium niobate ($LiNbO_3$) chip. Fig. 13(a) shows a cross section of the x-cut crystal with titanium (Ti) diffused waveguides. They are orientated along the z-axis of the crystal to create a nearly isotropic waveguide. The voltage V_B creates a horizontal electric field E_y in the waveguide, the voltage V_C generates a vertical field E_x. The center electrode is also biased by $V_B/2$ because it is situated half way between the outer electrodes. If the waveguide is ideally isotropic the propagation constants β_{TE} and β_{TM} for the TE- and TM-modes, respectively, are equal and complete TE/TM-coupling can be achieved by a vertical electric field E_x [35] with the coupling coefficient

$$\kappa \sim n_0^3 \cdot r_{61} \cdot E_x. \tag{14}$$

The horizontal field E_y leads to a difference in the propagation constants

$$\delta = (\beta_{TE} - \beta_{TM})/2 \sim n_0^3 \cdot r_{22} \cdot E_y. \tag{15}$$

Both electric fields are applied simultaneously and the double azimuth d_2 of the linear retarder is given by

$$\tan(d_2) = \kappa/\delta \sim E_x/E_y. \tag{16}$$

The retardation is determined by

$$d_1 = 2 \cdot \sqrt{\kappa^2 \cdot \delta^2} \cdot L \tag{17}$$

where L is the electrode length. From (16) and (17) follows

$$E_y \sim d_1 \cdot \cos(d_2) \tag{18}$$

$$E_x \sim d_1 \cdot \sin(d_2). \tag{19}$$

It is easily understood that the control voltages will not overflow, no matter which values d_2 assumes. Mathematical errors in the control system are prevented if d_2 is always chosen in the periodic range 0 to 2π. If the point $d_1 = 0$ is passed and negative d_1 occurs, d_2 is (mathematically) switched over by π and the negative d_1 sign is inverted. Only if d_1 exceeds the range limit π, a kind of reset including control voltage changes is necessary. d_2 is incremented or decremented by about π until d_1 returns from the range limit. (It should be pointed out that even both input and output SOP may vary if the d_1 range is chosen from 0 to 2π instead, whereas the reset remains the same.)

Some intrinsic TE/TM modal birefringence appears even in isotropic crystals due to the different reflection conditions at the crystal–superstrate interface for TE and TM modes. This birefringence can be compensated by a static horizontal field component E_y. Another possibility would be to orient the waveguides by a small angle relative to the z-axis of the crystal, thereby eliminating the modal birefringence [36].

In fabricated IO devices a submicron lateral electrode misalignment is unavoidable. The orthogonal electrical field components consequently depend on both applied voltages.

C. Experiments with a System Containing Two Integrated Optical Linear Retarders

In the experimental setup, a 1300-nm laser feeds several meters of single-mode fiber including manual SOP controllers (Fig. 13(b)). The fiber is affixed to the IO chip which contains two retarders. The output beam passes through the SOP analyzer and is focused on a photodetector. The controller closes the feedback loop as usual.

The IO retarders appeared to be less accurate than fiber squeezers, largely due to the strong reflections at the chip facets which we did not attempt to eliminate. Part of the light is reflected back and undergoes different SOP transformations. If it is again reflected and travels in the original direction, it can modify the generated SOP as a function of the chip length or temperature, thus introducing nonideal behavior and drift.

Our adjustment algorithm optimizes the overall function including input SOP and control voltages. The critical point is the reset at $d_1 = \pi$. From (13) it follows that the generated SOP is independent from d_2 (cf., Fig. 12). In a real device, the output SOP will at least describe movements near the Poincaré sphere pole L. The amplitude d_{max} of these deviations (in radians) may easily be determined, if the analyzed SOP is set equal or orthogonal to the center of these movements. For reasons of accuracy we choose the orthogonal analyzer position.

During the optimization procedure d_2 is varied in a ramp or saw-tooth pattern from 0 to 2π. The maximum intensity I_{max} is automatically recorded. It is comparable to the losses of the system during the reset at $d_1 = \pi$. From (4) follows

$$I_{max} = \sin(d_{max}/2)^2. \quad (20)$$

The input and analyzed SOP as well as the control voltage parameters are now alternatively varied in small steps in the direction of decreasing I_{max}. It was experimentally verified that this optimization converged well. The result with $d_1 = \pi$ and $I_{max} = 0.05$ is shown in Fig. 14. The control voltages were

$$V_B = -34.7\ \text{V} + 15.7\ \text{V/rad} \cdot d_1 \cdot \cos(d_2) \quad (21)$$

$$V_C = -13.3\ \text{V} + 7.5\ \text{V/rad} \cdot d_1 \cdot \sin(d_2 - 0.34\ \text{rad}). \quad (22)$$

In a real endless SOP control system the intensity losses will be higher than I_{max}, e.g., because the SOP analyzed during the reset will not be equal to the position found during the optimization procedure. For this reason the residual output SOP aberrations were corrected by the second retarder (parameters d_1', d_2'). Its control voltages V_B' and V_C' were optimized as described above. d_1', d_2' are polar coordinates as in (18), (19), (21), (22). They were substituted by the Cartesian coordinates

$$d_3 + f_3(d_2) \cdot d_1/\pi = d_1' \cdot \cos(d_2') \quad (23)$$

$$d_4 + f_4(d_2) \cdot d_1/\pi = d_1' \cdot \sin(d_2'). \quad (24)$$

The periodic nonlinear functions $f_3(d_2)$ and $f_4(d_2)$ are shown in Fig. 15 for $d_2 = 0$ to 2π, $d_3 = d_4 = 0$. The criterion for recording the functions is that $I = 0$ must be reached for the current d_2 value. If the optimization procedure converges well, the pattern describes several loops and may roughly be circumscribed by a circle of radius d_{max} centered at the origin. The weights d_1/π make $f_3(d_2)$ and $f_4(d_2)$ fully functional at $d_1 = \pi$ and suppress them at $d_1 = 0$. The meridians $d_2 = \text{const.}$ of the corrected output SOP on the Poincaré sphere will therefore only intersect at the points $d_1 = 0$ and $d_1 = \pi$.

With nonlinear correction the intensity deviations of Fig. 14 are reduced below $I_{max} = 0.01$. However, during longer periods, a rising I_{max} indicated a 0.3-rad drift of the output SOP. The additional control parameters d_3 and d_4 overcome the problem and make the system error-tolerant. As the second retarder is situated at the output, d_3 and d_4 are mainly functional during the reset near $d_1 = \pi$, and near $d_1 = 0$.

In our experiments the intensity is again minimized to assess losses accurately. The control parameters d_1 to d_4 are independently modulated. Integral controllers let d_1 and d_2 assume any values whereas d_3 and d_4 are kept near zero by proportional first order low-pass controllers. In Fig. 16(a) and (b) the polarizer turns once, which in each case means two turns on the Poincaré sphere. The control

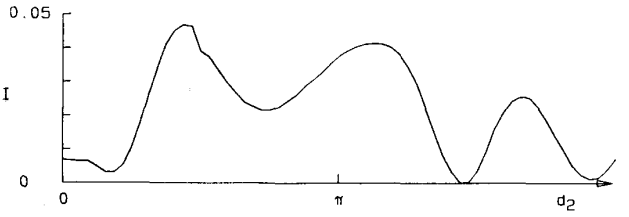

Fig. 14. Remaining intensity after parameter optimization at $d_1 = \pi$.

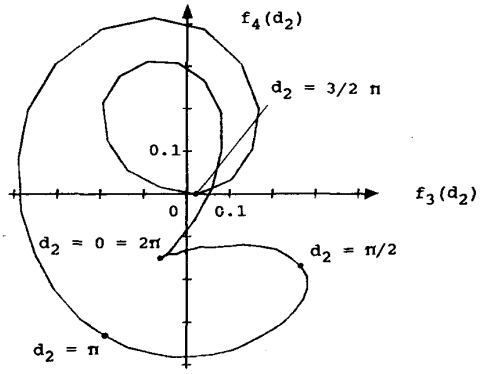

Fig. 15. Plot of the nonlinear SOP corrections $f_3(d_2)$ and $f_4(d_2)$ by the second retarder.

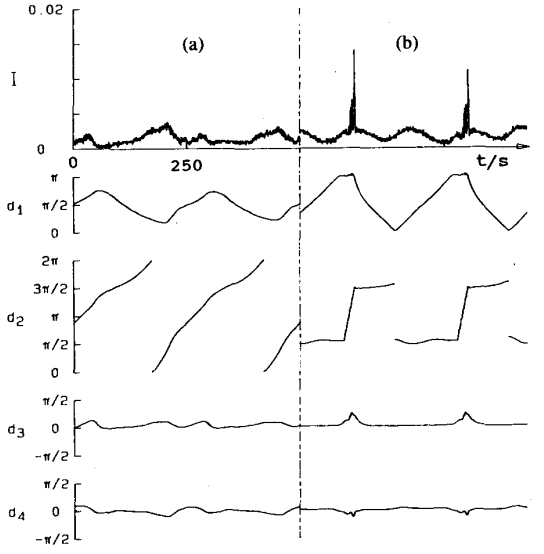

Fig. 16. Endless SOP control with rotating polarizer where the points $d_1 = 0$ and $d_1 = \pi$ (a) are not touched and (b) are touched.

voltages perform periodic movements. In Fig. 16(a) the Poincaré sphere circle described by the analyzed SOP does not touch the poles and the d_2 range is endless. The intensity losses of less than 0.005 were caused by our limited tracking speed and would approach zero if the analyzer movement were stopped. In Fig. 16(b), the quarter-wave plate is set so that the analyzed SOP passes the critical reset point and its antipode. At $d_1 = 0$, d_2 is

switched over by π which, according to (18), (19), and (21)–(24), means no control voltage change. At $d_1 = \pi$. d_2 is slowly changed by about π. Thus d_1 returns from the range limit. The retardations d_3 and d_4 correct arising SOP mismatch almost completely. The intensity losses stay below 0.1 dB ($\triangleq$ 0.02 which adds to the modulation losses of 0.05 dB.

IV. Conclusion

Automatic endless SOP control is an important method of achieving continuous polarization matching in coherent optical systems or sensors. It is more difficult to realize than conventional SOP control. However, several practical systems with only negligible intensity losses and reasonable tracking speeds have been demonstrated. In our experiments, a desktop computer served as feedback-controller and the SOP transformer consisted either of fiber squeezers or integrated optical devices. Real integrated optical retarders may be idealized by nonlinear correction. Error-tolerance at the expense of a somewhat reduced tracking speed seems to be an important system requirement. It makes time variant or nonideal device characteristics tolerable. The system with integrated optical devices is well suited to coherent optical communication.

Acknowledgment

The authors are indebted to G. Lohr for designing the initial versions of controlling hardware and software. They are grateful to Prof. H. Marko at the Technical University of Munich, where part of this work was carried out. They thank Dr. K. Panzer, Siemens AG Munich, for providing the semiconductor laser. They gratefully acknowledge the permission to publish this paper.

References

[1] Y. Yamamoto, "Receiver performance evaluation of various digital optical modulation-demodulation systems in the 0.5 to 10μm wavelength region," *IEEE J. Quantum Electron.*, vol. QE-16, no. 11, pp. 1251–1259, 1980.

[2] T. Okoshi *et al.*, "Computation of bit-error-rate of various heterodyne and coherent-type optical communications schemes," *J. Optical Commun.*, vol. 2, pp. 89–96, 1981.

[3] R. E. Wagner, "Coherent optical systems technology," in *Proc. 12th ECOC*, 1986, vol. 3, pp. 71–78.

[4] J. L. Gimlett, R. S. Vodhanel, M. M. Choy, A. F. Elrefaie, N. K. Cheung, and R. E. Wagner, "2-Gbit/s 101-km optical FSK heterodyne transmission experiment," presented at OFC/IOOC, 1987, pap. PDP11, pp. 44–47.

[5] A. H. Gnauck, R. A. Linke, B. L. Kasper, K. J. Pollock, K. C. Reichmann, R. Valenzuela, and R. C. Alferness, "Coherent lightwave transmission at 2 Gbit/s over 170 km of optical fiber using phase modulation," *Electron. Lett.*, vol. 23, no. 6, pp. 286–287, 1987.

[6] R.-P. Braun, R. Ludwig, and R. Molt, "Ten-channel coherent optic fiber transmission using an optical traveling wave amplifier," in *Proc. ECOC*, 1986, vol. 3, pp. 29–32.

[7] R. Ulrich, "Polarization stabilization on single-mode fiber," *Appl. Phys. Lett.*, vol. 35, no. 11, pp. 840–842, 1979.

[8] R. Noé, "Entwurf und Aufbau von unterbrechungsfreien Polarisations nachführungen im optischen Überlagerungsempfang," dissertation, Technical University of Munich, West Germany, 1987.

[9] B. Glance, "Polarization independent coherent optical receiver," *J. Lightwave Technol.*, vol. LT-5, no. 2, pp. 274–276, 1987.

[10] D. Kreit and R. C. Youngquist, "Polarization-insensitive optical heterodyne receiver for coherent FSK communications," *Electron. Lett.*, vol. 23, no. 4, pp. 168–169, 1987.

[11] T. Okoshi and Y. H. Cheng, "Four-port homodyne receiver for optical fiber communications comprising phase and polarization diversities," *Electron. Lett.*, vol. 23, no. 8, pp. 377–378, 1987.

[12] T. G. Hodgkinson, R. A. Harmon, and D. W. Smith, "Polarization-insensitive heterodyne detection using polarization scrambling," *Electron. Lett.*, vol. 23, no. 10, pp. 513–514, 1987.

[13] Y. Sasaki *et al.*, "26-km-long polarization-maintaining optical fiber," *Electron. Lett.*, vol. 23, no. 3, pp. 127–128, 1987.

[14] R. Noe, "Endless polarization control system with three finite elements of limited birefringence ranges," *Electron. Lett.*, vol. 22, no. 25, pp. 1341–1343, 1986.

[15] R. Noe, "Error-tolerant endless polarization control system with negligible signal losses for coherent optical communications," in *Proc. 13th ECOC*, 1987, vol. 1, pp. 371–374.

[16] R. Noe, "Endless polarization control in coherent optical communications," *Electron. Lett.*, vol. 22, pp. 772–773, 1986.

[17] R. M. A. Azzam and N. M. Bashara, *Ellipsometry and Polarized Light*. Amsterdam, The Netherlands: North-Holland, 1977.

[18] G. N. Ramachandran and S. Ramaseshan, "Crystal Optics," in *Handbook of Physics*, vol. 25/1, S. Flügge, Ed. Berlin: Springer, 1962.

[19] M. Johnson, "In-line fiber-optical polarization transformer," *Appl. Opt.*, vol. 18, no. 9, pp. 1288–1289, 1979.

[20] F. Mohr and U. Scholz, "Active polarization stabilization systems for use with coherent transmission systems or fibre-optic sensors," in *Proc. ECOC*, 1983, pp. 313–316.

[21] H. Heidrich, C. H. v. Helmolt, D. Hoffmann, H.-P. Nolting, H. Ahlers, and A. Kleinwächter, "Polarization transformer with unlimited range on Ti:$LiNbO_3$," in *Proc. 12th ECOC*, 1986, vol. 1, pp. 411–414.

[22] H. Heidrich, C. H. v. Helmolt, D. Hoffmann, H. Ahlers, A. Kleinwächter, "Integrated optical compensator on Ti:$LiNbO_3$ for continuous and reset-free polarization control," in *Proc. 13th ECOC*, 1987, vol. 1, pp. 257–260.

[23] R. Noé, "Endless polarization control for heterodyne/homodyne receivers," in *Proc. Fiber Optics SPIE*, 1986, vol. 630, pp. 150–154.

[24] R. Noé and G. Fischer, "17.4-Mbit/s heterodyne data transmission at 1.5-μm wavelength with automatic endless polarization control," in *Proc. Opto*. Paris, France: ESI, 1986.

[25] N. G. Walker and G. R. Walker, "Endless polarization control using four fibre squeezers," *Electron. Lett.*, vol. 23, no. 6, pp. 290–292, 1987.

[26] L. J. Rysdale, "Method of overcoming finite-range limitation of certain state of polarization control devices in automatic polarization control schemes," *Electron. Lett.*, vol. 22, no. 2, pp. 100–102, 1986.

[27] C. J. Mahon and G. D. Khoe, "'Compensational deformation': New endless polarization matching control schemes for optical homodyne or heterodyne receivers which require no mechanical drivers," in *Proc. 12th ECOC*, 1986, vol. 1, pp. 267–270.

[28] V. Thomas, "Optimierung eines Polarisations-Regelalgorithmus," Diploma thesis, Institute for Telecommunications, Technical University, Munich, 1987.

[29] H. C. Lefevre, "Single-mode fiber fractional wave devices and polarisation controllers," *Electron. Lett.*, vol. 16, pp. 778–780, 1980.

[30] T. Okoshi *et al.*, "New polarization-state control device: Rotatable fiber cranks," *Electron. Lett.*, vol. 21, pp. 895–896, 1985.

[31] T. Matsumoto *et al.*, "400-Mbit/s long-span optical FSK transmission experiment at 1.5 μm," *Proc. IOOC-ECOC*, 1985, vol. 3, pp. 31–34.

[32] T. Matsumoto and H. Kano, "Endlessly rotatable fractional-wave devices for single-mode-fibre optics," *Electron. Lett.*, vol. 22, no. 2, pp. 78–79, 1986.

[33] Peng Gangding, Huang Shangyuan, Lin Zonggi, "Application of electrooptic frequency shifters in heterodyne interferometric systems," *Electron. Lett.*, vol. 22, pp. 1215–1216, 1986.

[34] F. Heisman and R. Ulrich, "Integrated-optic single-sideband modulator and phase shifter," *IEEE J. Quantum Electron.*, vol. QE-18, no. 4, pp. 767–771, 1982.

[35] S. Thaniyavarn, "Wavelength independent, optical damage immune z-propagation $LiNbO_3$ waveguide polarization converter," *Appl. Phys. Lett.*, vol. 47, pp. 674–677, 1985.

[36] C. H. v. Helmolt, "Broad-band single-mode TE/TM convertors in $LiNbO_3$: A novel design," *Electron. Lett.*, vol. 22, pp. 155–156, 1986.

Reinhold Noé was born May 6, 1960, in Darmstadt, W. Germany. In 1984 he graduated from the Technical University of Munich, W. Germany, with the Dipl.Ing. degree.

He worked at the Institute for Telecommunication on coherent optical communication with a special interest in polarization problems. In 1987 he received the Dr.-Ing. (Ph.D.) degree from the Technical University Munich. In 1987 he moved to Siemens AG. Munich, to complete work on integrated optical devices. From September 1987 to August 1988 he is with Bellcore, Red Bank, NJ.

*

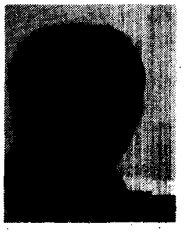

Helmut Heidrich received the Dipl.Phys. degree and the Dr.-Ing. degree from the Technical University Berlin, W. Germany, in 1973 and 1979, respectively.

From 1979 to 1982 he was with Standard Elektrik Lorenz AG., Berlin, first working in the innovation and development department in the area of digitally stored speech for application in public network offices, and finally heading a group developing intelligent system units for a public television system. In 1982 he joined the Integrated Optics Group at the Heinrich-Hertz-Institut für Nachrichtentechnik Berlin GmbH. He is currently heading a group doing R&D work on integrated optical lithium niobate components.

*

Detlef Hoffmann received the Dipl.Phys. degree from the University of Frankfurt/M. in 1978 and the Dr.-Ing. degree from the Ruhr-Uniersität in Bochum in 1983 where he began to work in the integrated optics field.

In 1982 he joined the Integrated Optics Group at the Heinrich-Hertz-Institut für Nachrichtentechnik Berlin GmbH where he is engaged in research and development in the field of integrated optical components on lithium niobate.